UC Berkeley
UC Berkeley Previously Published Works

Title
Bearing system health condition monitoring using a wavelet cross-spectrum analysis technique

Permalink
https://escholarship.org/uc/item/3d02p3md

Journal
Journal of Vibration and Control, 18(7)

ISSN
1077-5463

Authors
Liu, Jie
Wang, Wilson
Ma, Fai

Publication Date
2012-06-01

DOI
10.1177/1077546311417276

Peer reviewed

eScholarship.org Powered by the California Digital Library
University of California

Check for updates

Article

Journal of Vibration and Control
18(7) 953–963
© The Author(s) 2011
Reprints and permissions:
sagepub.co.uk/journalsPermissions.nav
DOI: 10.1177/1077546311417276
jvc.sagepub.com

Bearing system health condition monitoring using a wavelet cross-spectrum analysis technique

Jie Liu[1], Wilson Wang[2] and Fai Ma[3]

Abstract

Rolling-element bearings are widely used in rotary machinery systems. Accordingly, a reliable bearing fault detection technique is critically needed in industries to prevent the machinery system's performance degradation, malfunction, or even catastrophic failures. Bearing fault detection, however, still remains a very challenging task because most of the bearing fault related signatures are non-stationary. In this paper, a wavelet cross-spectrum (WCS) technique is proposed to tackle the challenge of feature extraction from these non-stationary signatures for bearing fault detection. The vibration signals are first analyzed by a wavelet transform to demodulate primary representative features; the periodic features are then enhanced by cross-correlating the resulting wavelet coefficient functions over several contributive neighboring wavelet bands. A Jarque-Bera statistic index is suggested for the bandwidth selection. The effectiveness of the proposed technique is examined by a series of experimental tests corresponding to different bearing conditions. Test results show that the developed WCS technique is an effective signal processing approach for not only stationary but also non-stationary feature extraction and analysis, and it can be applied effectively for bearing fault detection.

Keywords

Fault detection, feature extraction, rolling element bearing, signature analysis, vibration

Received: 16 January 2011; accepted: 3 June 2011

1. Introduction

Rolling element bearings are commonly used in various types of rotary machines. The development of reliable bearing health condition monitoring and failure prognostic techniques has been the focus of various undertakings in a wide array of industries to prevent machinery performance degradation, malfunction, or even catastrophic failures (Li et al., 1999; Patil et al., 2008; Timmins, 1998; Zhang et al., 2009, 2011). Bearing condition monitoring usually involves two sequential processes: feature extraction and fault diagnosis. Feature extraction is a process in which health condition related features are extracted by appropriate signal processing techniques (Timusk, et al., 2008); whereas fault diagnosis is a decision-making process to estimate bearing health conditions based on the extracted representative features (Liu et al., 2010). Therefore, feature extraction plays the key role for bearing health condition monitoring, whereas non-robust features may lead to false alarms (i.e., an alarm is triggered by some noise instead of a real bearing fault) or missed alarms (i.e., the monitoring tool cannot recognize the existence of a bearing defect) in diagnostic operations (Wang et al., 2004).

Several techniques have been proposed in the literature for bearing fault-related feature extraction, in which the analysis can be performed in the time domain (Heng and Nor, 1998), the frequency domain (Stack et al., 2006), or the time-frequency domain

[1]Department of Mechanical and Aerospace Engineering, Carleton University, Canada
[2]Department of Mechanical Engineering, Lakehead University, Canada
[3]Department of Mechanical Engineering, University of California, Berkeley, USA

Corresponding author:
Jie Liu, Department of Mechanical and Aerospace Engineering, Carleton University, Ottawa, ON, K1S 5B6, Canada
Email: jliu@mae.carleton.ca

(Li et al., 2008). In time-domain analysis, for example, a bearing fault is detected by monitoring the variation of some statistical indices such as root-mean-square value, crest factor or kurtosis. A bearing is believed to be damaged if the monitoring indices exceed predetermined thresholds; however, it is usually challenging to determine robust thresholds in real-world applications. Frequency-domain analysis is based on the transformed signal in the frequency domain. The advantage of frequency-domain analysis over time-domain analysis is its capability to easily identify and isolate certain spectral components of interest (Jardine et al., 2006). Bearing health conditions are assessed by examining the fault-related characteristic frequency components in a spectrum (Su and Lin, 1992) or in some extended spectral expressions such as bispectrum or cepstrum maps (Stack et al., 2004; Choi and Kim, 2007). Frequency-based techniques are usually supplemented with certain signal analysis methods to enhance representative spectral components, which include frequency filters, envelope analysis (McFadden and Smith, 1984), and modulation sidebands analysis (Blankenship and Singh, 1995; Sheen, 2007). Classical frequency-domain techniques, however, are not suitable for the analysis of non-stationary signatures that are generally related to machinery defects. Non-stationary or transient signatures can be analyzed by applying time-frequency domain techniques such as the short-time Fourier transform (FT) (Kaewkongka et al., 2003), Wigner-Ville distribution (Kim et al., 2007), cyclostationary analysis (Li and Qu, 2003; McCormick and Nandi, 1998), or wavelet transform (WT) (Wang et al., 2001). In bearing fault diagnosis, the WT is a favorite technique, because it does not contain such cross terms as those in the Wigner-Ville transform, while it can provide a more flexible multi-resolution solution than the short-time FT. According to signal decomposition paradigms, the WT can be classified as the continuous WT (Wang et al., 2004), discrete WT (Al-Raheem et al., 2008), wavelet packet analysis (Ocak and Loparo, 2005), and those WT with post-processing schemes such as the singularity analysis (Sun and Tang, 2002), the FT (Wang and Gao, 2003) and the energy density analysis (Cheng et al., 2005). A good review of the available methods for bearing fault diagnostics can also be found in Jardine et al. (2006) and Tandon and Choudhury (1999).

If a bearing is damaged, the generated vibration signals could be either stationary or non-stationary. It is relatively easier to analyze the stationary signals using some classical fault detection techniques, such as FT-based spectral analyses (Patil et al., 2008; Su and Lin, 1992).

However, it still remains a challenging task to extract robust representative features from the non-stationary vibration signals (e.g., those generated from a fault on bearing rotating components), particularly in real-world industrial applications (Su and Lin, 1992). This is because: 1) a bearing is a system instead of a simple mechanical component, which consists of inner/outer rings as well as a number of rolling elements; 2) slippage often occurs between the rolling elements and rings in operations; and 3) the machinery operation conditions are usually noisy. Correspondingly, the objective of this paper is to develop a new approach, called wavelet cross-spectrum (WCS) technique, to tackle this challenge in which the representative periodic features will be enhanced by an integration process over several contributive wavelet bands.

The rest of this paper is organized as follows. The proposed WCS technique is described in Section 2. Experimental tests are conducted in Section 3 to verify the effectiveness of the proposed technique, whereas some concluding remarks are summarized in Section 4.

2. The Wavelet Cross-spectrum (WCS) Technique

Whenever a fault occurs on a bearing component, impacts are generated in operation, which in turn excite the bearing and its support structures. The resulting resonance signatures are usually amplitude modulated by the bearing defect (McFadden and Smith, 1984); therefore, the analysis of these resonance signatures plays a key role in vibration-based bearing fault detection. Figure 1(a) shows part of a typical acceleration signal, measured from the housing of a tested bearing with an inner-race defect when the shaft speed f_t is 35 Hz. The experimental apparatus is illustrated in Section 3. When a defect occurs on a bearing rotating component, the modes and magnitudes of the resulting resonances often vary over time due to the variation in angular position of the impacts (Liu et al., 2008). This non-stationary characteristic of condition-related signatures makes bearing fault detection still a very challenging task in both research and industrial applications. In this work, a WCS technique is proposed as an alternative approach to investigate the characteristics of these non-stationary resonance signatures for the purpose of bearing fault detection. The WCS technique involves five steps for signal processing, which will be elaborated as follows. Some overlaps in content with Liu et al. (2008) have been maintained to ensure completeness and readability.

The first step is to apply the WT to demodulate the resonance vibration signatures, both stationary and non-stationary, over a series of wavelet bands. Given a continuous signal $x(t)$, the wavelet coefficients can be determined by

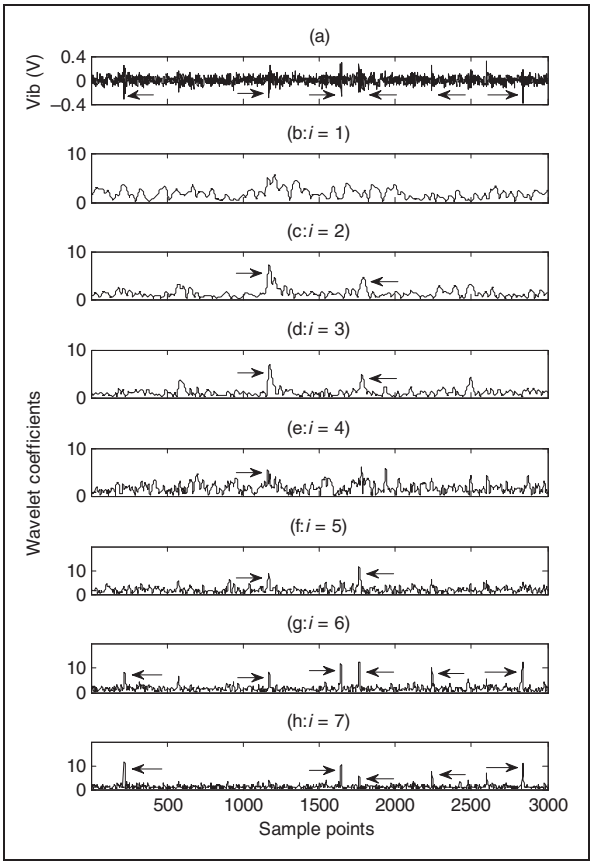

Figure 1. (a) Part of an acceleration signal generated by a bearing with an inner-race defect; (b) to (h) The normalized wavelet coefficients obtained from the vibration signal over seven wavelet bands ($i = 1, 2, \ldots, 7$).

$$W(t,s) = \int_{-\infty}^{+\infty} x(\tau)\,\sqrt{s}\,w^*(s(\tau - t))\,\mathrm{d}\tau, \qquad (1)$$

where $w^*(t)$ denotes the complex conjugation of mother wavelet function $w(t)$; s and t are the scale and time variables, respectively, which produce dilation and translation (Liu et al., 2008).

The choice of an appropriate mother wavelet depends on the signal properties and the purpose of the analysis. By testing and comparison, Morlet wavelet is selected as the mother wavelet for the signal analysis in this work (Liu et al., 2008; Ozturk et al., 2008; Strang and Nguyen, 1996):

$$w(t) = \exp\left(-\frac{t^2}{2b_0^2}\right)\exp(j2\pi f_0 t), \qquad (2)$$

where b_0 is the spread of the Gaussian function and f_0 is the center frequency of the pass-band of the mother wavelet. As $b_0 f_0$ increases, the duration of the wavelet expands, and the time resolution will decrease correspondingly. As a result, the obtained mother wavelet $w(t)$ may not be suitable to analyze fast-decaying transient signatures. To solve this problem, the product of the spread and the scaled center frequency is kept as a constant in this work (Liu et al., 2008), i.e.,

$$b_i f_i = \frac{b_0}{s_i}(f_0 s_i) = b_0 f_0 = \frac{1}{\sqrt{2\ln 2}}, \qquad (3)$$

where $2\pi b_0 f_0 = \pi\sqrt{2/\ln 2}$ was given in Strang and Nguyen (1996); s_i represents the ith selected scale; $b_i$and f_i are the corresponding ith spread and center frequency, respectively.

Based on the relation between b_i and f_i as in equation (3), the mean of the obtained mother wavelet $w(t)$ will be kept less than 10^{-12} in this case, and the effective support will vary with the scaled center frequency to accommodate the variation of the signatures of interest. At each wavelet scale s_i, the magnitude of wavelet coefficient function $|W(t,s_i)|$ that represents the demodulated envelope signal is normalized by its standard deviation, that is,

$$\overline{W}(t,s_i) = \frac{|W(t,s_i)|}{\left(\sum_{l=1}^{L}\left(|W(t_l,s_i)| - \frac{1}{L}\sum_{l=1}^{L}|W(t_l,s_i)|\right)^2/(L-1)\right)^{1/2}}, \qquad (4)$$

where $l = 1, 2, \ldots, L$, and L is the total number of samples; $i = 1, 2, \ldots, I$, and I is the number of wavelet scales; $|W(t_l,s_i)|$ is the lth sample of $|W(t,s_i)|$. To reduce the interference effects from the low-frequency noisy components, in this work, the overall frequency band of interest is chosen as $[Zf_t, f_s/2.56]$, where f_t denotes the shaft rotation speed, Z is the order of shaft harmonics of interest, Zf_t represents the lower bound frequency for feature extraction ($Z = 35$ is used in this case); f_s is the sampling frequency, and the constant 2.56 is selected to avoid aliasing effects (Girgis and Guy, 1988). The centre frequencies of the wavelet functions should be deployed properly to implement the WT over this designated frequency band $[Zf_t, f_s/2.56]$, without the overlapping between the wavelet frequency bands. Based on the FT of the dilated wavelet $w(st)$, the 3-dB bandwidth BW_i for the ith centre frequency f_i is derived from: $BW_i = [1-\lambda, 1+\lambda]f_i$, where $\lambda = \ln 2/\sqrt{2}\pi$ is a constant. Beginning with the lower bound frequency Nf_t, the centre frequencies f_i can be recursively calculated and positioned as (Liu et al., 2008):

$$f_i = \frac{(1+\lambda)^{i-1}}{(1-\lambda)^i} Zf_t,\ i = 1,\ 2,\ \ldots,\ I{-}1 \qquad (5)$$

$$f_i = \frac{1}{2}\left[\frac{f_s}{2.56} + f_{i-1}(1+\lambda)\right],\ i = I \tag{6}$$

where I is the number of the wavelet scales ($I = 7$ in this case). Figures 1(b) to (h) show the respective normalized wavelet coefficients $\overline{W}(t, s_i)$ over seven wavelet bands, which are determined based on the vibration signal as shown in Figure 1(a). It can be seen that the resonance signatures in Figure 1(a) are usually demonstrated in several consecutive wavelet bands (Figures 1(b) to (h)) due to the variation of the transient modes.

The second step to implement the proposed WCS technique is to cross-correlate the wavelet coefficient functions from the neighboring wavelet bands to enhance the defect-related periodic features, that is,

$$\begin{aligned} X_i(l) &= E[\bar{W}(t, s_i)\bar{W}^*(t+l, s_{i+1})] \\ l &= 0,\ 1,\ 2,\ \ldots, L-1;\ \mathrm{i} = 1,\ 2,\ \ldots., I-1. \end{aligned} \tag{7}$$

$$\bar{X}_i(l) = \frac{X_i(l) - \mu_i}{\sigma_i}, \tag{8}$$

where $E[\cdot]$ is the expectation function; $\bar{X}_i(l)$ are the cross-correlation sequences that are normalized by their standard deviation σ_i around the mean μ_i. In estimating the correlation sequence, the method proposed here is different from the commonly used Pearson's approach in which the product-moment correlation estimation limits $\bar{X}_i(l)$ to the range of [-1 1]. It is also noted that the cross-correlations are performed on the neighboring wavelet bands; this is because the demodulated features from the resonance signatures are usually reflected on the adjacent wavelet bands. An example is illustrated in Figure 1 where the extracted features are marked by arrows. From a physical perspective, each time as a bearing incipient fault encounters its mating components, an impact is generated, which in turn induces the resonance of the local structure.

Corresponding to each impulse, the resonant response usually occurs over consecutive frequency bands in a random nature. Figures 2(a) to (f) illustrate the $\bar{X}_i(l)$ array determined from six pairs of neighboring wavelet bands. It is seen that some periodic features are prominent (e.g., in Figures 2(b), (e), and (f)) whereas others are less pronounced (e.g., in Figures 2(a), (c), and (d)). Correspondingly, another key process in bearing incipient fault detection is how to properly choose the more contributive wavelet bands so as to highlight the periodic features.

Each periodic feature with high amplitudes will modify the distribution of correlation sequence and cause the distribution more skewed and heavily-tailed, which will be characterized by the Jarque-Bera (JB) statistic (Croux et al., 2006; Gel et al., 2007) in this work. The correlation coefficient from each pair of neighboring wavelet bands is treated as a discrete random variable, and its probability distribution is then examined. As an example, Figures 2(a') to (f') show the probability distributions of the correlation sequences in the corresponding Figures 2(a) to (f). It is seen that the properties of the tails of the distribution function vary with respect to its bandwidth. To characterize this effect, a JB statistic-based performance index J_i is proposed as:

$$J_i = \frac{1}{6}\left[S_i^2 + \frac{(K_i - 3)^2}{4}\right],\ \mathrm{i} = 1,\ 2,\ \ldots., I-1. \tag{9}$$

where S_i and K_i are, respectively, the skewness and kurtosis that are estimated by using a large number of samples ($L = 327{,}680$ in this case). The proposed statistic index J_i can characterize the abnormality present in the distribution of correlation sequence by incorporating the information from both the skewness and the kurtosis, and both heavily-tailed and heavily-skewed distributions would increase the index J_i. In bearing fault detection, a larger J_i is expected when the bearing is faulty, since it indicates that the periodic features are highlighted (i.e., with higher magnitudes). Accordingly, the third step in the implementation of the WCS technique is to choose more contributive bandwidths in which the correlation sequences could bring about larger J_i. Figure 3 shows the values of the index J_i, $i = 1, 2, \ldots, 6$, corresponding to the correlation sequences shown in Figures 2(a) to (f). It is seen that correlation sequences #2, #5, and #6 generate greater index J_i.

The fourth step of the proposed WCS technique is to integrate the correlation coefficient functions from the contributive bandwidths to achieve a 1-D representation. In this work, a J-weighted function is suggested for the integration process:

$$\begin{aligned} H(l) &= \frac{\sum_{m \in C} J_i \bar{X}_i(l)}{\sum_{m \in C} J_i}, \\ I &= 1, 2, \ldots, L;\ C \subset \{1, 2, \ldots, I-1\} \end{aligned} \tag{10}$$

where C is a subset of $\{1,\ 2, \ldots, I-1\}$. The selection of the members of C depends on applications; in this case, C takes the top half of the members of $\{1,\ 2, \ldots, I-1\}$ whose corresponding correlation sequences generate greater J_i. Figure 4(a) shows some examples of the integrated correlation sequence $H(l)$ derived using equation (10). It is seen that the periodic features, carried by the vibration signal in Figure 1(a), can be clearly recognized. These periodic features are spaced by an interval of 118 samples, or with the repetition rate of approximately 173 Hz (i.e., the

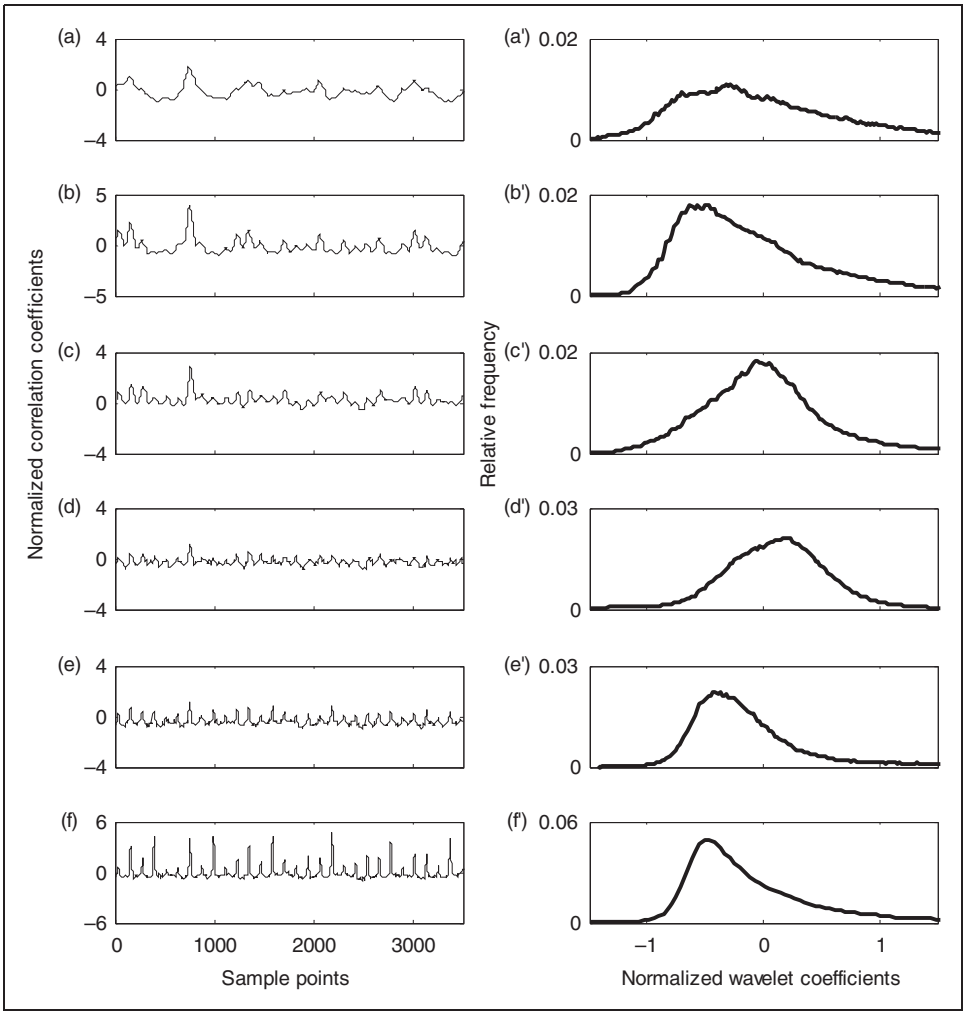

Figure 2. (a) to (f) The zero-mean normalized correlation sequences determined from six pairs of neighboring wavelet bands. (a') to (f') The probability distribution functions of the resulting cross correlation sequences corresponding to six pairs of neighboring wavelet bands; the probability is evaluated by using its relative frequency of occurrence with 500 bins and 327680 sample points.

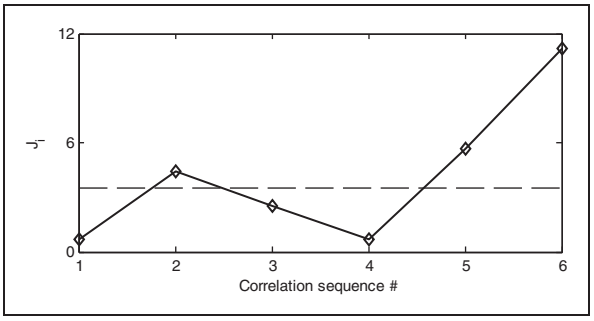

Figure 3. The performance index J_i corresponding to different correlation sequences.

inner-race defect frequency) for a sampling frequency of 20480 Hz.

Once the integrated cross correlation sequences are obtained, the fifth (or the final) step is to examine the characteristic defect frequencies (i.e., the inner race defect frequency f_{id}, the outer race defect frequency f_{od}, and the rolling element defect frequency f_{ed} (Stack et al., 2004)) from the averaged autocorrelation spectrum. This autocorrelation spectrum analysis involves two processes (Liu et al., 2008): performing the autocorrelation on $H(l)$ to further enhance the involved periodic features, and conducting the spectral analysis for periodic feature extraction. Specifically,

$$r(\kappa) = E[H(l)H^*(l+\kappa)],\ \kappa = 0,\ 1,\ 2,\ \ldots,\ L-1 \quad (11)$$

$$R(f) = F[r(\kappa)], \quad (12)$$

$$\Phi(f) = R(f)R^*(f), \quad (13)$$

where $F[\cdot]$ denotes the FT. In implementation, the spectra obtained by equation (13) from P segments of measured signals ($P = 5$ in this case) should be

normalized and averaged to reduce the effects of random noise,

$$\bar{\Phi}(f) = \frac{1}{P}\sum_{p=1}^{P} \frac{\Phi_p(f)}{\max\left(\Phi_p(0),\ \cdots,\ \Phi_p(f_u)\right)}, \qquad (14)$$

where f_u is the observation upper-bound frequency that should be larger than the maximum bearing characteristic frequency (Du and Yang, 2006; McFadden and Smith, 1984), and $f_u = 300$ Hz in this case. Bearing health conditions are estimated by analyzing the related characteristic frequency components (i.e., f_{id}, f_{od}, and f_{ed}) in the resulting spectra. Figure 4(b) demonstrates an example of the resulting spectra determined by the proposed WCS technique on the vibration signal shown in Figure 1(a). It is seen that the defect frequency (approximately 173.17 Hz) can be clearly recognized; in this case, the defect occurs on the bearing's inner race, that is, $f_{id} = 173.17$ Hz when the shaft speed $f_t = 35$ Hz.

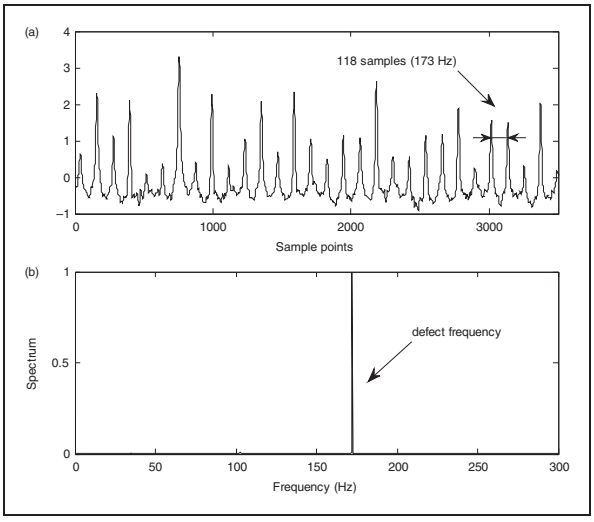

Figure 4. (a) The integrated correlation sequence $H(l)$; (b) the processing results of the bearing inner-race fault detection by using the wavelet cross-spectrum technique.

3. Performance validation

A series of tests have been conducted to verify the effectiveness of the proposed WCS technique in bearing fault detection; the experimental setup that is employed for these tests is shown in Figure 5. The shaft is driven by a 3-hp induction motor. The motor speed ranges from 20 rpm to 4200 rpm, which is manipulated by a speed controller. An optical sensor is used to provide a one pulse per revolution signal for rotation speed detection. A flexible coupling is employed to damp out high-frequency vibrations generated by the motor. The rolling element bearing under examination is press-fitted into the left bearing housing, and the vibration signals are measured by two accelerometers (ICP-IMI, SN98697) installed on the housing along both the horizontal and vertical directions. Radial loads are applied by two pairs of disks. A data acquisition board (NI PCI-4472) is employed for signal collection.

In the tests, four bearing health conditions are examined: healthy bearings, bearings with outer race defects, bearings with inner race defects, and bearings with rolling element faults. Each bearing is tested under seven

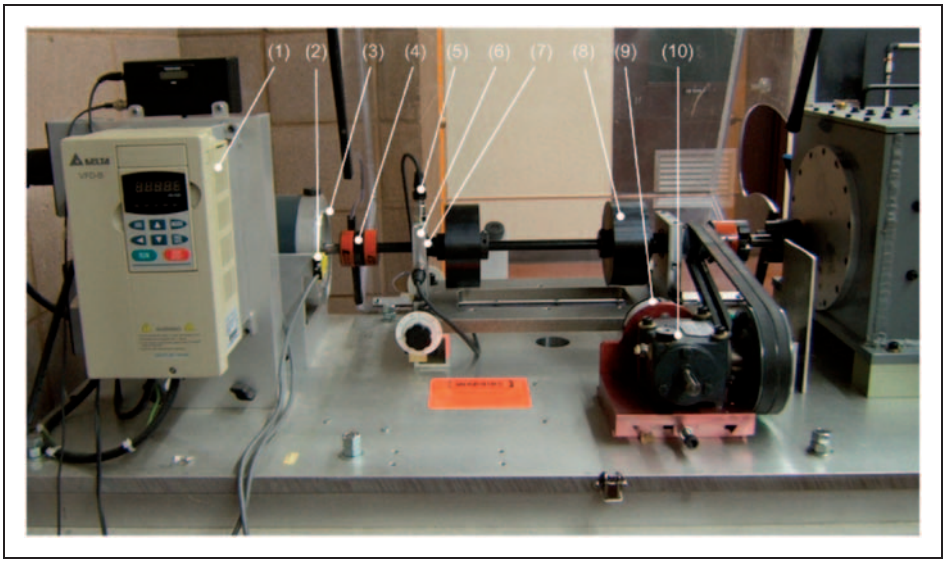

Figure 5. The experimental setup: (1)-speed control; (2)-optical sensor; (3)-motor; (4)-flexible coupling; (5)-ICP accelerometer; (6)-bearing housing; (7)-test bearing; (8)-load disc (the heavy load); (9)- magnetic load system; (10)-bevel gearbox.

shaft speeds (900, 1200, 1500, 1800, 1920, 2100, and 2400 rpm) and two load levels, respectively. The sampling frequency f_s is set at 20480 Hz.

The performance of the proposed WCS technique will be compared with two related classical methods, the one-scale WT (Wang and Gao, 2005) and the envelope demodulation-based FT (McFadden and Smith, 1984), to verify its effectiveness in non-stationary feature extraction and bearing incipient fault detection. In this comparison study, the classical methods are applied on both structural resonance frequency bands and entropy-based preselected frequency bands (Shi et al., 2004). In resonance frequency band investigation, the one-scale WT is employed with the wavelet center frequency at 2000 Hz; the envelope demodulation-based FT is conducted with the signal that is band-pass filtered around the resonant frequency [1500 2500] Hz of the bearing and housing (Liu et al., 2008). Preselected frequency bands are determined by using the Shannon entropy-based approach (Shi et al., 2004). The analysis of these two aforementioned classical methods is also based on the corresponding averaged autocorrelation spectra.

In frequency-based bearing fault detection, the bearing health is assessed by checking if there exists a pronounced spectral component in the resulting spectra, which corresponds to one of the bearing characteristic defect frequencies. If direct spectral examination cannot reveal clear fault detection information, as stated before, some supplementary methods should be properly employed to improve the diagnostic accuracy (Al-Raheem et al., 2008; Liu et al., 2010). In our investigation, it is found that when the bearing is in its normal condition, the shaft speed dominates the resulting spectra due to unavoidable imperfections (e.g., system unbalance). When an incipient bearing fault (i.e., inner race defect or outer race defect) occurs, the bearing characteristic defect frequency will become pronounced if the proposed WCS technique is employed. The results from these examinations are summarized in Table 1, in which the numbers represent the percentages of successful bearing health condition estimation. The criterion for the successful bearing condition estimation is given as follows: for a healthy (or normal) bearing, shaft speed should dominate the corresponding spectral map (or with the highest spectral magnitude); for a bearing with an inner/outer race defect, the corresponding characteristic defect frequency should be clearly recognized in the resulting spectra. From Table 1, it is seen that: 1) in general, the classical methods with entropy-based frequency band selection can be more reliable in detecting a bearing fault than those methods focusing only on structural resonance frequency band; 2) the proposed WCS outperforms these two classical methods in terms of bearing fault diagnostic accuracy, no matter which frequency band is examined. In the following context, the processing results from a typical testing case will be used as an example to illustrate bearing fault detection processes using different techniques.

3.1. Healthy bearing

As mentioned earlier, when the bearing is in its normal condition, the shaft speed dominates the resulting spectra due to some unavoidable shaft imperfections (e.g., unbalance) and the varying compliance (Tandon and Choudhury, 1999). For example, Figures 6(a) to 10(a) show the respective processing results from these three methods for a healthy bearing ($f_t = 35$ Hz). It is seen that the shaft speed can be clearly recognized by using the WCS technique (Figure 6(a)). By contrast, the shaft speed information cannot be clearly identified by using the one-scale WT and the envelope demodulation-based FT (Figures 7(a), 9(a) and 10(a)); instead, the third harmonic of the shaft speed dominates the resulting spectra (Figures 7(a) and 8(a)). As a matter of fact, this frequency may result in false diagnosis since its value is very close to the outer race defect frequency ($f_{od} = 106.83$ Hz in this case).

3.2. Outer race fault detection

An outer race defect is relatively easier to detect because the outer ring is fixed and the defect-related resonance modes do not change over time dramatically.

Table 1. Comparison of diagnostic results using different techniques

	One-scale WT	Envelope demodulation-based FT	One-scale WT (preselected scale)	Envelope demodulation-based FT (preselected frequency band)	WCS
Healthy bearing	64.3%	71.4%	50.0%	64.3%	100%
Bearing with outer race defect	85.7%	85.7%	92.9%	85.7%	100%
Bearing with inner race defect	50.0%	57.1%	78.6%	92.9%	92.9%

FT: Fourier transform; WCS: wavelet cross-spectrum; WT: wavelet transform.

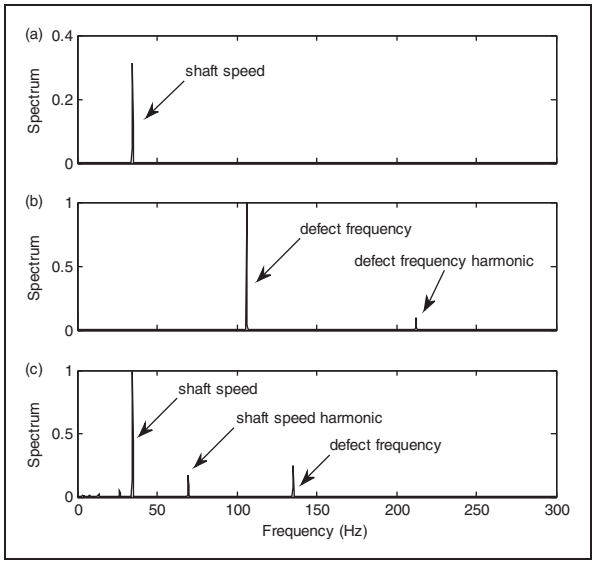

Figure 6. The processing results when the wavelet cross-spectrum technique is applied ($f_t = 35$ Hz): (a) healthy bearing; (b) bearing with an outer race fault; (c) bearing with a rolling element fault.

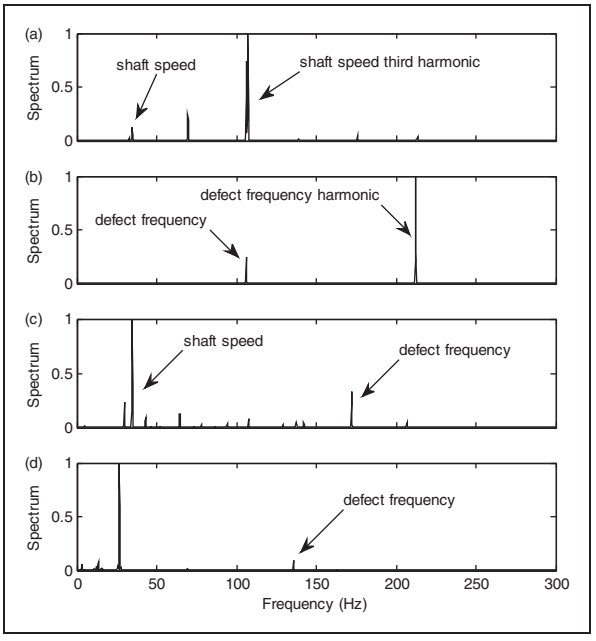

Figure 7. The processing results when the one-scale wavelet transform is applied on the structural resonance frequency band ($f_t = 35$ Hz): (a) healthy bearing; (b) bearing with an outer race fault; (c) bearing with an inner race fault; (d) bearing with a rolling element fault.

As illustrated in Table 1, the proposed WCS technique can detect the outer race faults in all test cases in which the outer race defect frequency are clearly recognized in the resulting spectra; one example is shown in

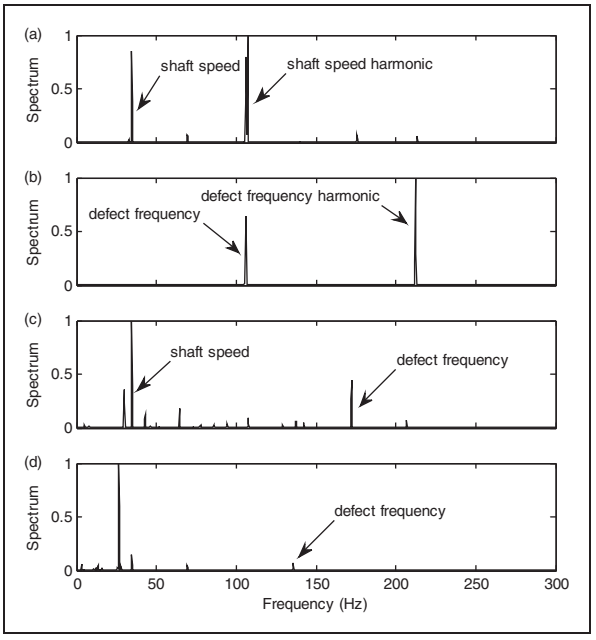

Figure 8. The processing results when the envelope demodulation-based Fourier transform is applied on the structural resonance frequency band ($f_t = 35$ Hz): (a) healthy bearing; (b) bearing with an outer race fault; (c) bearing with an inner race fault; (d) bearing with a rolling element fault.

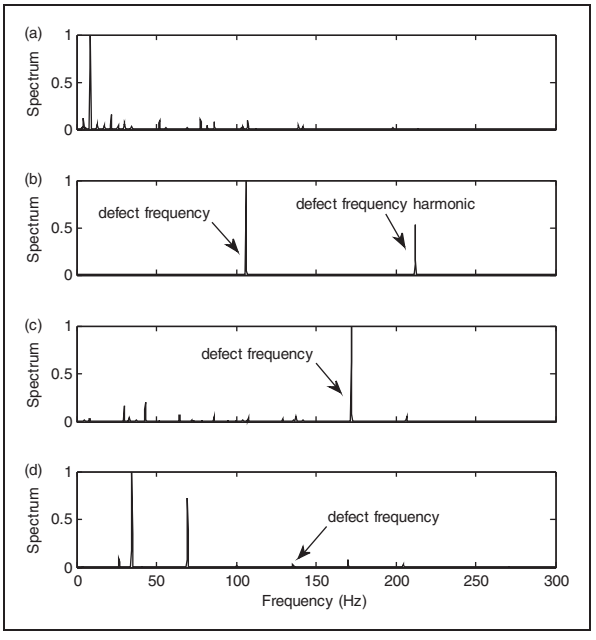

Figure 9. The processing results when the one-scale wavelet transform is applied on the entropy-based preselected frequency band ($f_t = 35$ Hz): (a) healthy bearing; (b) bearing with an outer race fault; (c) bearing with an inner race fault; (d) bearing with a rolling element fault.

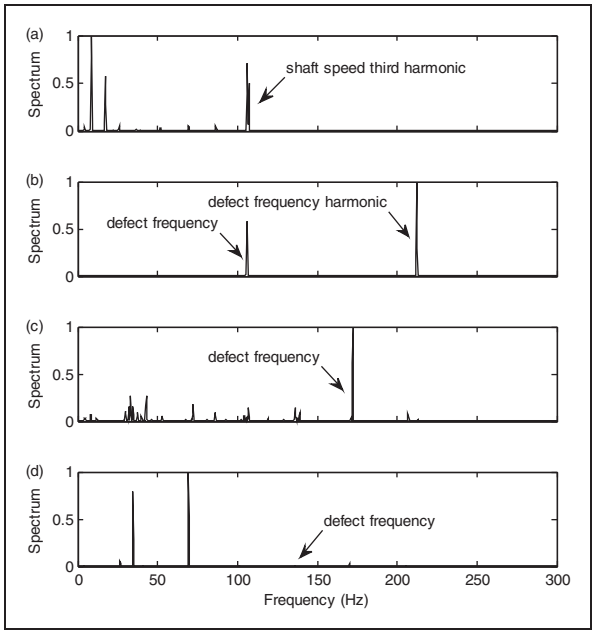

Figure 10. The processing results when the envelope demodulation-based Fourier transform is applied on the entropy-based preselected frequency band ($f_t = 35$ Hz): (a) healthy bearing; (b) bearing with an outer race fault; (c) bearing with an inner race fault; (d) bearing with a rolling element fault.

Figure 6(b) when $f_{od} = 106.83$ Hz. It is noted that the one-scale WT and the envelope demodulation-based FT technique can also detect the outer race defects although the dominant spectral component may be a harmonic of the outer race defect frequency, as seen in Figures 7(b), 8(b) and 10(b).

3.3. Inner race fault detection

The detection of a fault on an inner race is more challenging than on a fixed outer ring because the modes of the generated resonance signatures vary over time. Test results in Table 1 demonstrate that the WCS technique is more reliable (e.g., Figure 4(b)) than the related classical methods (e.g., Figures 7(c) to 10(c)) in detecting bearing faults on rotating rings and in suppressing the noisy spectral components. This is because the WCS technique is capable of integrating the periodic features from several contributive wavelet bands. The performance of the related classical methods is improved when the frequency bands are determined by using the Shannon entropy analysis (e.g., Figures 9(c) and 10(c)). It is also interesting to see that the sidebands of the shaft speed around the inner race frequency harmonics can be slightly observed in Figures 7(c) to 10(c), but can hardly be recognized in Figure 4(b). As a matter of fact, the sidebands of the shaft speed around the inner race harmonics physically exist in Figure 4(b); however, because the proposed WCS technique can make the inner race defect frequency more dominant and prominent in the resulting spectra, consequently these sidebands cannot be clearly recognized from the corresponding spectral map.

3.4. Rolling element fault detection

The detection of a rolling element fault for ball bearings is one of the most challenging tasks in bearing health condition monitoring, especially when the fault is at its initial stage. This is because: a) the resonance signatures generated by a ball defect are non-stationary; and b) the impacts are random since the defect may not always strike the races. In our tests, it is found that the rolling element defect frequency can be detected as long as the shaft speed is sufficiently high (e.g., over 30 Hz in this test), although the related defect spectral component is not the dominant one in the resulting spectra. It is also seen that the defect frequency processed by using the WCS technique (e.g., Figure 6(c)) is more prominent than those from the two classical methods (e.g., Figures 7(d) to 10(d)). In this case, the diagnostic reliability could be improved by integrating information from other fault detection techniques such as the time-domain kurtosis ratio approach (Liu et al., 2010).

4. Conclusion

A WCS technique is proposed in this paper for representative feature extraction and bearing incipient fault detection. The WCS technique performs feature extraction by demodulating the non-stationary resonance signatures generated by bearing incipient defects and then correlating the periodic patterns over more contributive wavelet bands. A JB statistic-based performance indicator is suggested to guide the wavelet band selection. The effectiveness of the proposed WCS technique is verified by a series of experiments corresponding to different bearing conditions. Test results show that the WCS technique is an effective approach for non-stationary feature extraction and bearing fault detection. It outperforms the related classical methods such as one-scale WT and the envelope demodulation-based FT.

Acknowledgements

The authors would like to thank the reviewers for their valuable suggestions.

Funding

This work was supported by Natural Sciences and Engineering Research Council of Canada (NSERC) and Carleton University.

References

Al-Raheem KF, Roy A, Ramachandran KP, Harrison DK and Grainger S (2008) Application of the Laplace-wavelet combined with ANN for rolling bearing fault diagnosis. *ASME Journal of Vibration and Acoustics* 130: 1–9.

Blankenship GW and Singh R (1995) Analytical solution for modulation sidebands associated with a class of mechanical oscillators. *Journal of Sound and Vibration* 179: 13–36.

Cheng J, Yu D and Yang Y (2005) Time-energy density analysis based on wavelet transform. *NDT & E International* 38: 569–572.

Choi YC and Kim YH (2007) Fault detection in a ball bearing system using minimum variance cepstrum. *Measurement Science and Technology* 18: 1433–1440.

Croux C, Dhaene G and Hoorelbeke D (2006) Testing the information matrix equality with robust estimators. *Journal of Statistical Planning and Inference* 136: 3583–3613.

Du Q and Yang S (2006) Improvement of the EMD method and applications in defect diagnosis of ball bearings. *Measurement Science and Technology* 17: 2355–2361.

Gel YR, Miao W and Gastwirth JL (2007) Robust directed tests of normality against heavy-tailed alternatives. *Computational Statistics & Data Analysis* 51: 2734–2746.

Girgis A and Guy B (1988) A computer based data acquisition system for teaching transients and switching phenomena and performing research on digital protection. *IEEE Transactions on Power Systems* 3: 1361–1368.

Heng RBW and Nor MJM (1998) Statistical analysis of sound and vibration signals for monitoring rolling element bearing condition. *Applied Acoustics* 53: 211–226.

Jardine A, Lin D and Banjevic D (2006) A review on machinery diagnostics and prognostics implementing condition-based maintenance. *Mechanical Systems and Signal Processing* 20: 1483–1510.

Kaewkongka T, Au YHJ, Rakowski RT and Jones BE (2003) A comparative study of short time Fourier transform and continuous wavelet transform for bearing condition monitoring. *International Journal of COMADEM* 6: 41–48.

Kim BS, Lee SH, Lee MG, Ni J, Song JY and Lee CW (2007) A comparative study on damage detection in speed-up and coast-down process of grinding spindle-typed rotor-bearing system. *Journal of Materials Processing Technology* 187: 30–36.

Li FC, Meng G, Ye L and Chen P (2008) Wavelet transform-based higher-order statistics for fault diagnosis in rolling element bearings. *Journal of Vibration and Control* 14(11): 1691–1709.

Li L and Qu L (2003) Cyclic statistics in rolling bearing diagnosis. *Journal of Sound and Vibration* 267: 253–265.

Li Y, Billington S, Zhang C, Kurfess T, Danyluck S and Liang S (1999) Adaptive prognostics for rolling element bearing condition. *Mechanical Systems and Signal Processing* 13: 103–113.

Liu J, Wang W and Golnaraghi F (2008) An extended wavelet spectrum for bearing fault diagnostics. *IEEE Transactions on Instrumentation and Measurement* 57: 2801–2812.

Liu J, Wang W and Golnaraghi F (2010) An enhanced diagnostic scheme for bearing condition monitoring. *IEEE Transactions on Instrumentation and Measurement* 59: 309–321.

McCormick AC and Nandi AK (1998) Cyclostationarity in rotating machine vibrations. *Mechanical Systems and Signal Processing* 12: 225–242.

McFadden PD and Smith JD (1984) Vibration monitoring of rolling element bearings by the high-frequency resonance technique-a review. *Tribology International* 17: 3–10.

Ocak H and Loparo KA (2005) HMM-based fault detection and diagnosis scheme for rolling element bearings. *ASME Journal of Vibration and Acoustics* 127: 299–306.

Ozturk H, Sabuncu M and Yesilyurt I (2008) Early detection of pitting damage in gears using mean frequency of scalogram. *Journal of Vibration and Control* 14(4): 469–484.

Patil M, Mathew J and Rajendrakumar P (2008) Bearing signature analysis as a medium for fault detection: a review. *ASME Journal of Tribology* 130: 1–7.

Sheen YT (2007) An analysis method for the vibration signal with amplitude modulation in a bearing system. *Journal of Sound and Vibration* 303: 538–552.

Shi DF, Wang WJ and Qu LS (2004) Defect detection for bearings using envelope spectra of wavelet transform. *ASME: Journal of Vibration and Acoustics* 126: 567–573.

Stack JR, Habetler TG and Harley RG (2006) Fault-signature modeling and detection of inner-race bearing faults. *IEEE transactions on Industry Applications* 42: 61–68.

Stack JR, Harley RG and Habetler TG (2004) An amplitude modulation detector of fault diagnosis in rolling element bearings. *IEEE Transactions on Industrial Electronics* 51: 1097–1102.

Strang G and Nguyen T (1996) *Wavelets and Filter Banks*. Wellesley MA: Wellesley-Cambridge Press.

Su YT and Lin SJ (1992) On initial fault detection of a tapered roller bearing: frequency domain analysis. *Journal of Sound and Vibration* 155: 75–84.

Sun Q and Tang Y (2002) Singularity analysis using continuous wavelet transform for bearing fault diagnosis. *Mechanical Systems and Signal Processing* 16: 1025–1041.

Tandon N and Choudhury A (1999) A review of vibration and acoustic measurement methods for the detection of defects in rolling element bearings. *Tribology International* 32: 469–480.

Timmins PF (1998) *Solutions to Equipment Failures*. Materials Park OH: ASM International.

Timusk M, Lipsett M and Mechefske CK (2008) Fault detection using transient machine signals. *Mechanical Systems and Signal Processing* 22: 1724–1749.

Wang C and Gao RX (2003) Wavelet transforms with spectral post-processing for enhanced feature extraction. *IEEE Transactions on Instrumentation and Measurement* 52: 1296–1301.

Wang W, Golnaraghi F and Ismail F (2004) Condition monitoring of a multistage printing press. *Journal of Sound and Vibration* 270: 755–766.

Wang W, Ismail F and Golnaraghi F (2001) Assessment of gear damage monitoring techniques using vibration

measurements. *Mechanical Systems and Signal Processing* 15: 905–922.

Wang W, Ismail F and Golnaraghi F (2004) A neuro-fuzzy approach for gear system monitoring. *IEEE Transactions on Fuzzy Systems* 12: 710–723.

Zhang B, Sconyers C, Patrick R and Vachtsevanos G (2009) A multi-fault modeling approach for fault diagnosis and failure prognosis of engineering systems. *In Proceedings of the International Conference on Prognostics & Health Management*, San Diego CA, Sept 27–Oct 1.

Zhang B, Sconyers C, Byington C, Patrick R, Orchard ME and Vachtsevanos G (2011) A probabilistic fault detection approach: application to bearing fault detection. *IEEE Transactions on Industrial Electronics* 58: 2011–2018.